Functional sample VV001/2020

The protocol for robust and efficient preparation of the self-blotting nanowire TEM grids

Authors:

Vít Vykoukal
Karolína Citterbardová
Jiří Nováček

CEITEC, Masaryk University

The functional sample was developed within the frame of Technological Agency of the Czech Republic project TN01000008

Content

1. Introduction …….. 2

2. The goal of the functional sample ……... 2

3. Functional sample description …… 3

4. Functional sample optimization procedure …… 4

5. Novelty of the functional sample …….. 7

6. Acknowledgements ……..…….. 7

7. References …….. 7

1. Introduction

Transmission electron microscopy of vitreous biological specimens (cryo-EM) has become a powerful tool in Structural Biology research over the last decade and is nowadays being recognized as one of the primary techniques in biology [Kuhlbrandt 2014; Nogales 2015]. The increased recognition is primarily due to technological developments which helped to overcome some of the limitations of earlier cryo-EM. These technological developments primarily comprise utilization of direct electron detection cameras (DEDs) [McMullan,Faruqi,Clare & Henderson 2014], development of stable transmission electron microscopes capable of long unsupervised data acquisition, and software tools for data analysis [Lyumkis,Brilot,Theobald & Grigorieff 2013; Punjani,Rubinstein,Fleet & Brubaker 2017; Zivanov et al. 2018]. In contrast, the mainstream technique for sample preparation has remained the same for more than 30 years [Dubochet et al. 1988]. The standard protocol applies 2.5 – 4 µl of the specimen to a TEM grid, followed by blotting 99.9% of the sample away with a filter paper, and plunge freezing the grid into the liquid ethane. Besides the fact that the majority of the specimen is wasted during preparation, it is very difficult to fully control the blotting process. Therefore, large numbers of grids are usually prepared for single followed by costly screening in order to find single grid which is suitable for cryo-EM data acquisition. The sample preparation is thus nowadays identified as the main step limiting throughput of cryo-EM. Recent developments of the instruments which deposit nl - pl amounts of the sample directly to the TEM grid without a need further sample blotting decreases sample amount and increases the reproducibility of the prepared cryo-EM samples [Razinkov et al. 2016; Arnold et al. 2017; Ravelli et al. 2020]. One of these devices is called “Spotiton” and its principle based on piezo-dispensing of the pl sample droplets to the specifically treated “nanowired” TEM grids [Razinkov et al. 2016]. The surface of the grid is coated with $Cu(OH)_2$ nanowires which wick away the excess of the liquid. Here, we present a protocol for robust and reproducible preparation of the TEM grids coated with Cu(OH)2 nanowires.

2. The goal of the functional sample

The document provides a protocol for preparation of the TEM grids coated with the $Cu(OH)_2$ nanowires. Such TEM grids are specifically suitable for preparation of the macromolecular samples for cryo-electron microscopy using spray of piezo-dispenzing devices.

3. Functional sample description

The 200-mesh or 300-mesh Au TEM grids were purchased from SPI (https://www.2spi.com/category/grids-au-square/grids-au/). The grids were washed for 10 minutes in acetone, 10 minutes in iso-propyl alcohol (IPA), and air-dried under ambient conditions on the glass slide for another 30 minutes. The grids were positioned such that the flat ("shiny") side was facing the glass slide. The glass slide with the grids was transferred to the Quorum Technologies Q150T ES sputter coater. The 57 x 0.25 mm Copper target (99.99% Cu) was mounted into the instrument and Cu sputtering was performed at 60 mA current under the Argon atmosphere for 30 minutes resulting in 700 nm of Cu on the top of the Au TEM grids. The sputter coater was equipped with the film thickness monitor which was used to calibrate the proper sputtering time. Subsequently, the TEM grids were transferred to the glow discharge unit (Quorum Technologies SC7620), an plasma cleaned in Ar:O2 (75:25) atmosphere for 2 minutes (7 mA, 7 Pa). The grids were then floated on the surface of a reaction mixture comprising 0.13 M ammonium persulfate and 2.5 M sodium hydroxide at pH 13.8 with the Copper side facing towards the liquid. The ammonium persulfate solution was always freshly prior to the experiment. The reaction was carried out for 20 s. $Cu(OH)_2$ nanowire synthesis is described by the equation

$$Cu + 4\,NaOH + \left(NH_4\right)_2 S_2 O_8 \rightarrow Cu\left(OH\right)_2 + 2\,Na_2 SO_4 + 2\,NH_3\uparrow + 2\,H_2 O \qquad (1)$$

The reaction was stopped by addition of high access of water. Subsequently, the grids were washed with ethanol for 10 minutes, another 10 minutes with 1:1 IPA:acetone, and dried under ambient conditions. The overall grid quality, the nanowire morphology and size was determined using FIB/SEM microscopy (Fig. 1).

The final TEM grids were uniformly covered with the 2.0 ± 0.3 um $Cu(OH)_2$ nanowires.

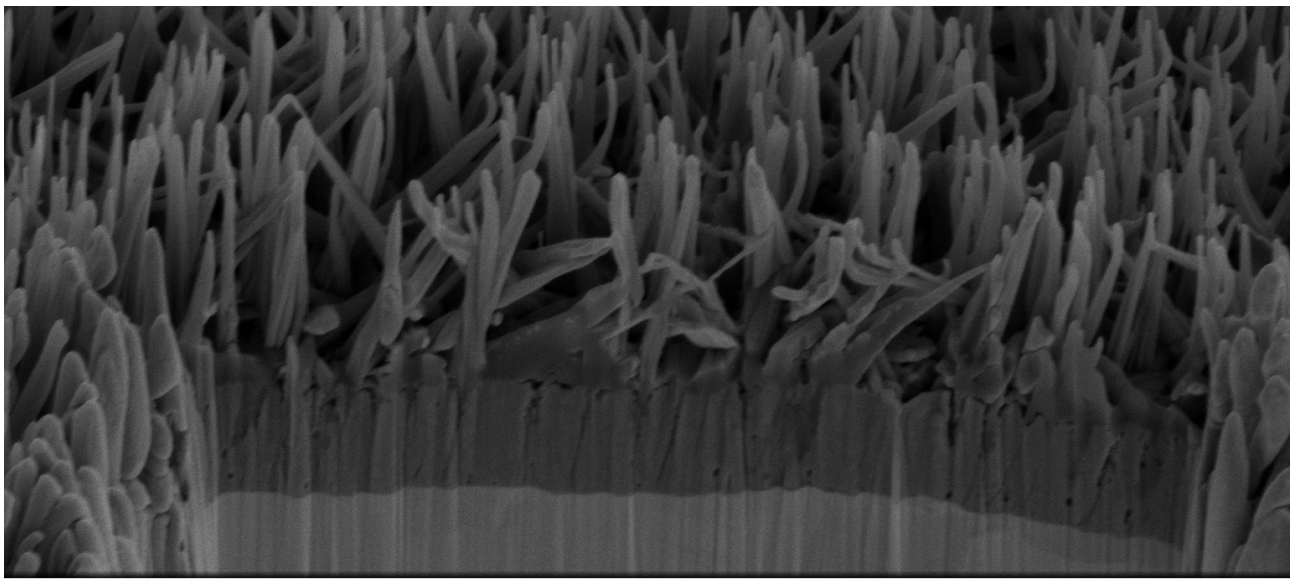

Fig. 1: Detail of the $Cu(OH)_2$ nanowires on the TEM grid. The cross-section through the grid bar was prepared using focused ion beam to facilitate nanowire size analysis. The layers of Au, Cu and $Cu(OH)_2$ nanowires can be clearly separated.

4. Functional sample optimization procedure

The final protocol for the $Cu(OH)_2$ nanowire grid preparation resulted from an optimization process where various parameters were systematically changed and its effect on the final product was monitored. Here, we summarize the major parameters which influence the quality of the nanowire grid preparation.

4.1 The reaction time determines nanowire length and characteristics

The reaction time (eq. 1) was incrementally increased for the TEM grids sputter coated with 700 nm Cu layer, and the morphology of the nanowires was studied in scanning electron microscope (SEM, Fig. 2). In order to determine the nanowire size distribution, a part of the nanowire coated grid bar was removed by a focused ion beam (FIB) which facilitated measurement of the nanowire length. The results are summarized in Table 1.

Interaction time [s]	Nanowire size range [nm]
10	720 – 1110
20	1790 – 2300
30	1100 – 2350
40	860 – 1500
50	840 – 1600
60	630 – 1510

Table 1: Dependence between the reaction time and nanowire size distribution for 700nm Cu layer.

The results in Table 1 reveal that there is an optimum reaction time for which the nanowires reach the maximum length and provide relatively narrow size distribution. The nanowire length distribution broadens with additional prolongation of the reaction time over the optimum (here 20 s) and the maximum size gradually decreases. The major reason for the decreasing nanowire size is the sintering of individual nanowires at the top side resulting in formation of aggregated compact layer at the grid surface (Fig. 2E,F). The sintering artifacts significantly decrease the surface of the grid and consequently its blotting capacity.

4.2 The thickness of the Cu layer influences distribution of the nanowire length

The effect of the Cu layer thickness on the nanowire characteristics was studied. We have found out that the nanowire growth is not initiated when the thickness of the sputtered layer is smaller than 200 nm. The maximal length of the nanowires increases with the increasing thickness of the sputter Cu layer. However, the variability in the nanowire size distribution also increases for the thicker Cu layers. This effect is summarized in Table 2 which shows the size distribution of the nanowires grown from the 1.4 μm thick Cu layer.

Interaction time [s]	Nanowire size range [nm]
30	600 – 2100
60	1060 – 4620
90	730 – 5240

Table 1: Dependence between the reaction time and nanowire size distribution for 1.4μm Cu layer.

The comparison with the data in Table 1 documents that even though the nanowires are significantly longer when grown from the 1.4 µm instead of 700 nm sputtered Cu layer. On the other hand, the distribution of the nanowire sizes also dramatically increases for the 1.4 µm layer and may diminish the reproducibility of the blotting capacity.

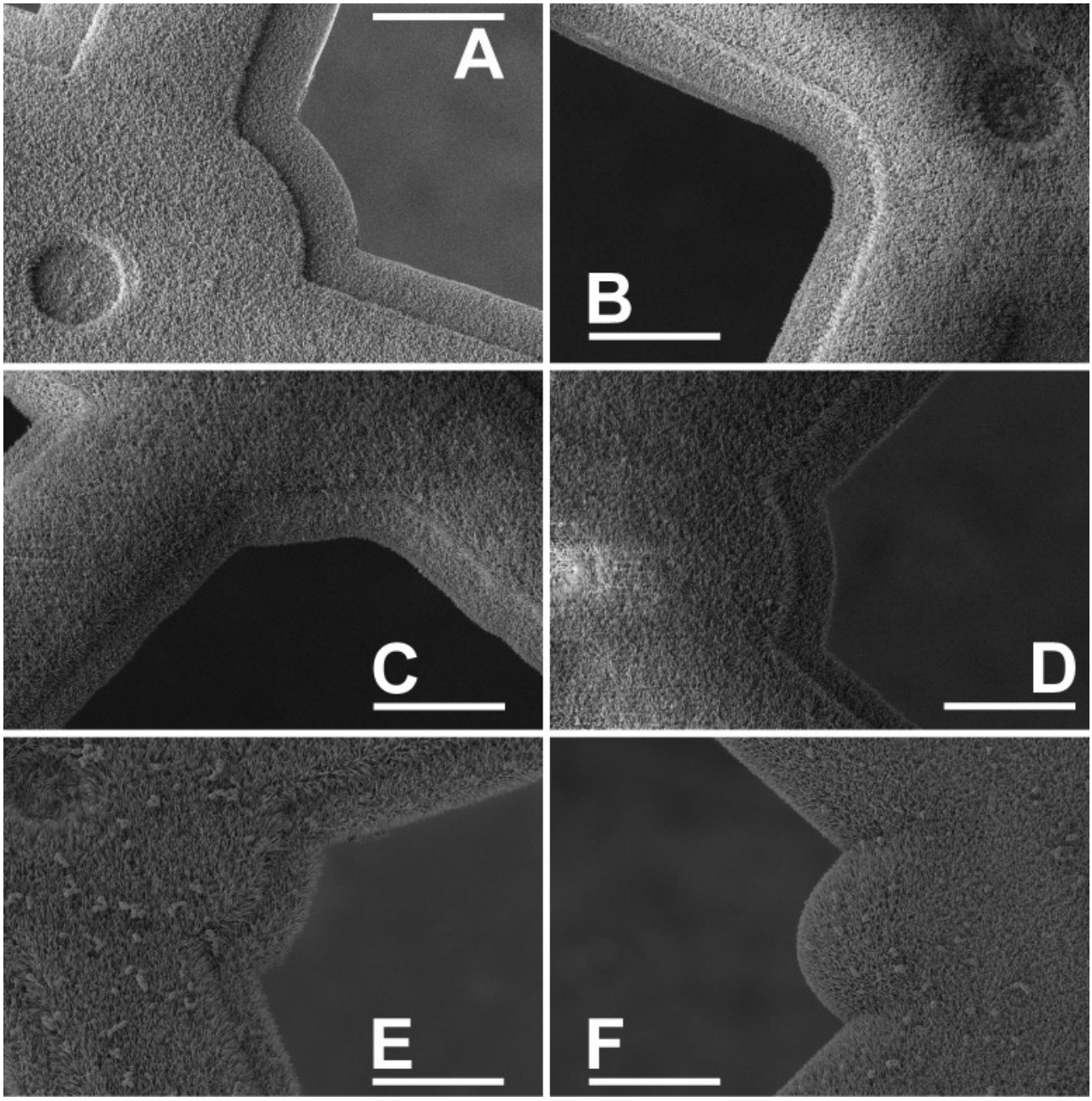

Fig. 2: Detail of the TEM grid with the $Cu(OH)_2$ nanowires developed after 10s (A), 20s (B), 30s (C), 40s (D), 50s (E), 60s (F) reaction. The scale bar represents 20µm.

5. Novelty of the functional sample

The functional sample provides a protocol for reproducible preparation of TEM grids coated with a uniform layer of $Cu(OH)_2$ nanowires. The novelty of the protocol stems in sputtering of Cu layer on Au TEM grids instead of utilization of TEM grids directly made of Cu which significantly improves the reproducibility of the results. In addition, we also provide a description of the main nanowire parameters which are determinant for the blotting capacity of the grid and describe conditions under which sintering artifacts appear.

6. Acknowledgements

This work was financially supported by TA CR (project TN01000008).

7. References

Arnold, S. A.; Albiez, S.; Bieri, A.; Syntychaki, A.; Adaixo, R.; McLeod, R. A.; Goldie, K. N.; Stahlberg, H. and Braun, T. (**2017**). *Blotting-free and lossless cryo-electron microscopy grid preparation from nanoliter-sized protein samples and single-cell extracts*, Journal of Structural Biology 197 : 220-226.

Dubochet, J.; Adrian, M.; Chang, J.-J.; Homo, J.-C.; Lepault, J.; McDowall, A. W. and Schultz, P. (**1988**). *Cryo-electron microscopy of vitrified specimens*, Quarterly Reviews of Biophysics 21 : 129-228.

Kuhlbrandt, W. (**2014**). *The Resolution Revolution,* Science 343 : 1443-1444.

Lyumkis, D.; Brilot, A. F.; Theobald, D. L. and Grigorieff, N. (**2013**). *Likelihood-based classification of cryo-EM images using FREALIGN*, Journal of Structural Biology 183 : 377-388.

McMullan, G.; Faruqi, A.; Clare, D. and Henderson, R. (**2014**). *Comparison of optimal performance at 300keV of three direct electron detectors for use in low dose electron microscopy*, Ultramicroscopy 147 : 156-163.

Nogales, E. (**2015**). *The development of cryo-EM into a mainstream structural biology technique*, Nature Methods 13 : 24-27.

Punjani, A.; Rubinstein, J. L.; Fleet, D. J. and Brubaker, M. A. (**2017**). *cryoSPARC: algorithms for rapid unsupervised cryo-EM structure determination*, Nature Methods 14 : 290-296.

Ravelli, R. B. G.; Nijpels, F. J. T.; Henderikx, R. J. M.; Weissenberger, G.; Thewessem, S.; Gijsbers, A.; Beulen, B. W. A. M. M.; López-Iglesias, C. and Peters, P. J. (**2020**). *Cryo-EM structures from sub-nl volumes using pin-printing and jet vitrification*, Nature Communications 11.

Razinkov, I.; Dandey, V. P.; Wei, H.; Zhang, Z.; Melnekoff, D.; Rice, W. J.; Wigge, C.; Potter, C. S. and Carragher, B. (**2016**). *A new method for vitrifying samples for cryoEM*, Journal of Structural Biology 195 : 190-198.

Zivanov, J.; Nakane, T.; Forsberg, B. O.; Kimanius, D.; Hagen, W. J.; Lindahl, E. and Scheres, S. H. (**2018**). *New tools for automated high-resolution cryo-EM structure determination in RELION-3*, eLife 7.